# Solving of Optimal Power Flow Problem Including Renewable Energy Resources Using HEAP Optimization Algorithm

**MOHAMED A. M. SHAHEEN**[ID]1, **HANY M. HASANIEN**[ID]2, **(Senior Member, IEEE)**,
**AND AHMED AL-DURRA**[ID]3, **(Senior Member, IEEE)**

1Electrical Engineering Department, Faculty of Engineering and Technology, Future University in Egypt, Cairo 11835, Egypt
2Electrical Power and Machines Department, Faculty of Engineering, Ain Shams University, Cairo 11517, Egypt
3Advanced Power and Energy Center, Department of Electrical Engineering and Computer Science, Khalifa University, Abu Dhabi 127788, United Arab Emirates

Corresponding author: Ahmed Al-Durra (ahmed.aldurra@ku.ac.ae)

**ABSTRACT** This paper presents a novel endeavor to use the Heap optimization algorithm (HOA) to solve the problem of optimal power flow (OPF) in the electricity networks. The key objective is to optimize the cost of fuel of the conventional generators under the system limitations. Various scenarios are studied in a later stage considering the addition of the PV panel and/or wind farm with changing load curves during a typical day. The active output power of the generators is selected to be the OPF problem search space. The HOA is employed to get the best solution of the fitness function and provides the corresponding best solutions. The modeling of the heap-based optimizer (HBO) depends on three levels: the relation between the subordinates and the boss, the relation between the same level employees, and the contribution of the employee oneself. The validity of the proposed algorithm is tested for a variety of electric grids, the IEEE 30-bus, IEEE 57-bus and 118 bus networks. These networks are simulated under various scenarios. Real load curves, in this study, are considered to achieve a practical outcome. The simulation outcomes are evaluated and tested. The results indicate that the implemented HOA-based OPF methodology is flexible and applicable compared with that achieved by using the genetic algorithm.

**INDEX TERMS** Optimal power flow, optimization, power systems, renewable energy.

## I. INTRODUCTION

### A. MOTIVATION AND INCITEMENT

Power systems are known as dynamic systems with a high degree of complexity. They consist of generation stations, transmission networks, and distribution networks that are owned and managed by companies or countries. The electric power transmission grids have some limitations while operation. These limitations emerge from issues about temperature, voltage and stability [1]. The OPF problem is a well-known nonlinear optimization problem. The main objective of the OPF optimization problem is to choose the optimal solution for the network or grid design variables that meet the minimum value of the objective function taking into account

the constraints of the electric power system. The active generator power, generator voltage, transformer taps settings or VAR compensators can be described as a design variable by the researchers. Generally, the OPF objective functions are categorized according to a single objective function or multi-objective functions. In the single objective function optimization problems, only one objective is targeted meanwhile in the multi-objective ones, many objectives are accomplished simultaneously. These targets can include the generators' fuel costs, the generators' emission rates, electricity loss in an electricity grid and the voltage security index.

### B. LITERATURE REVIEW

The OPF problem was dedicated by more than one traditional method in the literature survey like the Newton–Raphson [2], and the interior point method [3]. Orthodox

The associate editor coordinating the review of this manuscript and approving it for publication was S. Ali Arefifar[ID].

approaches typically suffer from several demerits. The initial problem guess that depends on the differential equation solver which is heavily impacted on them. Furthermore, because the OPF optimization problem is non-linear, the traditional methods can be kept in the local minimum point instead of the global minimum. Furthermore, the problems must be simplified by specifying mathematical assumptions. Therefore, to overcome such drawbacks and obstacles, it is necessary to find competent methods of optimization.

Different innovative metaheuristic methods are recently used to handle the OPF. These methods were successful in removing barriers of conventional mathematical methods. Particle swarm optimization (PSO) [4], grey wolf optimization and differential evolution [5], [6], tree-seed algorithm [7], sine-Cosine algorithm [8], sun-flower optimization (SFO) [9], [10], coyote optimization algorithm [11], harris-hawks optimization (HHO) [12], [13], cuttlefish algorithm [14], cuckoo search algorithm [15], whale-optimization algorithm (WOA) [16], gravitational-search [17], marine predators [18], and salp swarm algorithm [19]–[22] are naturally inspired and divided fundamentally in techniques based on swarms and population. They have both their own benefits and inconvenience individually [23]. These metaheuristic-based methods initiate hazardous candidates and achieve the best solution based on their operation.

A community of individuals who work for a shared purpose will not do so until they organize themselves into a hierarchy known as a Corporate Rank hierarchy (CRH). This is the idea of proposing a new optimization algorithm, which arranges the fitness of search agents in a hierarchy. As the heap data structure is used to map a CRH definition, the algorithm proposed is called a heap optimization algorithm (HOA). This algorithm was first introduced by Qamar Askari, Mehreen Saeed, and Irfan Younas in 2020 [24]. Regarding the modeling of the HOA mathematically, it consists of three pillars: the combination of subordinates with the direct supervisor, the relationship amongst peers and the employee's own participation. The results are either higher or similar to the other algorithms used in literature. The novel meta-heuristic algorithm is motivated by such social behaviors, since the extraordinary outcomes of human behavioral optimization methods have pushed the domain of evolutionary-based and swarm-based intelligence up to a higher level. The proposed algorithm smartly models three forms of worker behavior: for example, subordinates' interaction with their immediate head, colleague-to-work interaction and employee self-contribution. The proposed optimization method may be updated to handle number of problems with smart systems related to engineering, industry, research and business optimization. The HOA allows many real-life resource planning, manufacturing planification, automobile steering, network optimization, robotics track preparation, packaging issues, and intelligent systems architecture challenge to be solved.

Furthermore, The HOA is simple in design and implementation [24].

## C. CONTRIBUTION AND PAPER ORGANIZATION

The OPF remains active and continues with the use of these approaches as novel metaheuristic strategy development. It has multiple goals. It can be solved simultaneously and/or in sequence. The most common aim is to minimize the fuel cost of the generators. The HOA is used to deal with the OPF in this article. The proposed method is designed to minimize a single target within the network constraints. The research has in fact provided: (1) measurement of the proficiency and success of the HOA when handling the OPF in power systems compared with obtained using the genetic algorithm (GA), (2) optimum photovoltaic (PV) [25] and wind farm positioning [26] using the sunflower optimization (SFO) and the Harris Hawks Optimization (HHO) algorithm, and (3) impact of adding PV and/or wind turbines [27] on the cost of fuel in the OPF using the proposed HOA compared with the GA [28]. The goal is to minimize fuel prices. The algorithm adopted is used for evaluating the best values for the variables of the architecture regulation. The real output power of the generators is the OPF search space. The HOA is chosen for the OPF in the electric grids, the standard IEEE 30-, 57- and 118-bus systems considering many scenarios. Real load curves are considered in this analysis to achieve a practical outcome. The results of optimization are provided by MATLAB software, and the results obtained illustrate the HOA's competition to reach the OPF optimization problem solution with GA. The major contributions of this paper are: 1) Evaluation of the newly proposed HOA when applied to the OPF problem in its classical base case, 2) Investigating the effect of inserting renewable energy sources and load variation through a typical day of the objective function to be minimized.

The remaining sections of the paper are organized as follows: Section 2 presents the problem formulation. Section 3 presents the proposed algorithm employed for solving the OPF problem with different scenarios. Section 4 presents a discussion on the simulation results. Finally, the conclusion is presented in Section 5.

## II. FORMULATION OF THE OPF

Firstly, the goal is to make an assessment to the newly developed HOA with the help of the MATPOWER to run the OPF in the base case, without adding renewable energy sources and with fixed load, comparing the results with GA. Secondly, the optimum location where PV-panels are to be installed is decided by the SFO and HHO algorithms [9], [13]. The wind farm is positioned at an optimal bus. Thirdly, the OPF problem can be solved after only PV panels are inserted, only then a wind farm. Then, the OPF is tested concurrently with the addition of PV panels and wind farm. The networks that are used for this analysis, the standard IEEE 30-, 57-, and 118- bus systems.

## A. OPF WITH BASE CASE

The problem is an OPF single objective optimization problem. The following subsection clarifies it.

### 1) THE SINGLE OBJECTIVE

The prices charged by the energy services are the running costs of generators, which often cost of fuel during the operation. The cost function is defined in equations (1) and (2) as a quadratic function for the output active power [9].

$$Minimize \ J = \sum_{h=1}^{24} \sum_{i=1}^{NG} C_{i,h}\left(P_{Gi,h}\right) \tag{1}$$

$$C_{i,h}\left(P_{Gi,h}\right) = a_i * P_{Gi,h}^2 + b_i * P_{Gi,h} + c_i \tag{2}$$

where $J$ stands for the cost charged by the service provider, $NG$ represents the number of generators, and $P_{Gi,h}$ represents the real power at bus $i$ and moment $h$.

### 2) OPF PROBLEM CONSTRAINTS

The limitations of the OPF are expressed as shown in the following equations [9]:

$$P_{injk,h} - \sum_{l=1}^{N} V_{k,h} * V_{l,h} * \left[G_{kl} * \cos\left(\delta_{l,h} - \delta_{k,h}\right)\right.$$
$$\left. + B_{kl} * \sin\left(\delta_{l,h} - \delta_{k,h}\right)\right] = 0 \tag{3}$$

$$Q_{injk,h} - \sum_{l=1}^{N} V_{k,h} * V_{l,h} * \left[G_{kl} * \sin\left(\delta_{l,h} - \delta_{k,h}\right)\right.$$
$$\left. + B_{kl} * \cos\left(\delta_{l,h} - \delta_{k,h}\right)\right] = 0 \tag{4}$$

where: $P_{injk,h}$, $Q_{injk,h}$ represent the real and reactive power injected at bus $k$ at moment $h$ respectively, $V_{k,h}$ and $V_{l,h}$ represent the voltages of buses $k$ and $l$ at moment $h$. $G_{kl}$ and $B_{kl}$ represent the conductance and susceptance of $Y_{kl}$. $\delta_{l,h}$ and $\delta_{k,h}$ represent the voltage angles at buses $k$ and $l$ at hour $h$ respectively.

$$P_{Gmin} \leq P_{Gi,h} \leq P_{Gmax}, \ i = 1, 2, \ldots, NG \text{ and}$$
$$h = 1, 2, \ldots, 24 \tag{5}$$

$$Q_{Gmin} \leq Q_{Gi,h} \leq Q_{Gmax}, i = 1, 2, \ldots, NG \text{ and}$$
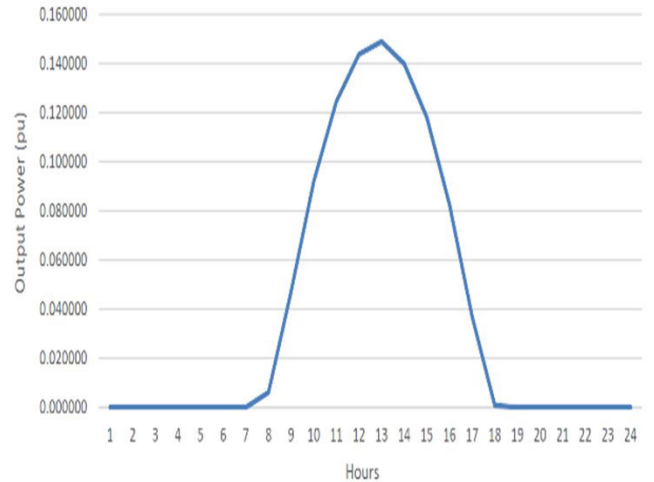$$h = 1, 2, \ldots, 24 \tag{6}$$

$$V_{imin} \leq V_{i,h} \leq V_{imax}, \ i = 1, 2, \ldots, NG \text{ and}$$
$$h = 1, 2, \ldots, 24 \tag{7}$$

$$\left| V_{k,h} * V_{l,h} * \left[G_{kl} * \cos\left(\delta_{l,h} - \delta_{k,h}\right)\right.\right.$$
$$\left.\left. + B_{kl} * \sin\left(\delta_{l,h} - \delta_{k,h}\right)\right]\right| \leq P_{limkl}, k,$$
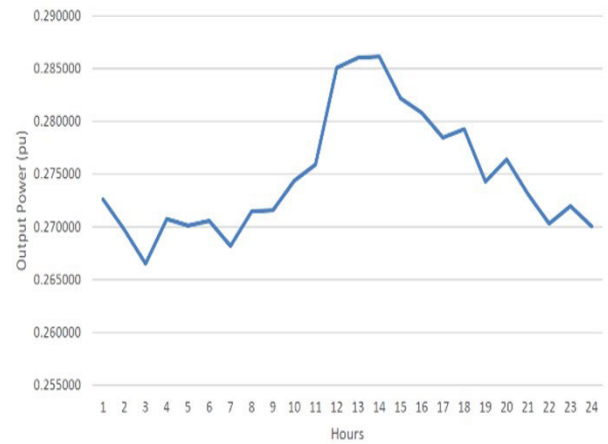$$l = 1, 2, \ldots, N \tag{8}$$

where $P_{limkl}$ represents the maximum power flow of a branch between nodes $k$ and $l$.

## B. TARGETING THE OPTIMAL BUSES OF THE RENEWABLE ENERGY SOURCES

The OPF is performed to add the PV panels starting trials at bus 2 until the end of the whole buses of each system, one at

(a)  PV panel output power.

(b)  Wind farm output power.

**FIGURE 1.** Hourly power provided by (a) PV panel, (b) Wind farm.

a time [9]. The bus that results in a lower cost for 24 hours is the best-chosen bus to add PV panels. The OPF is also run to optimize the wind farm location following the same strategy of the PV panel optimal siting, providing that the PV panel is mounted on the earlier chosen buses. In this study, the PV panel is selected to be of 15 MW capacity and the wind farm is 30 MW when studying the 30-bus system. For the 57-bus system, the added PV panel is selected to be of 90 MW capacity and the wind farm capacity is selected to be 175 MW. Finally, the PV added to the 118-bus system has a capacity of 300 MW while the added wind farm is a 575 MW one. These capacities are chosen to be comparable with the maximum demands of the test systems. In general, The PV panel and the wind farm produce a time varying electric power through the day [29], [30], [31]. The hourly power generated by the PV panel and the wind farm in a typical day in winter is shown in Fig. 1 [9].

## C. OPF INCLUDING VARIABLE LOADING CONDITIONS AND RENEWABLE ENERGY SOURCES

Following allocation of PV panels and wind turbines, the effects of incorporating these green energy sources on the overall cost of the OPF are evaluated in various scenarios. First of all, the only solar energy supplier is added to the OPF and then the only wind farm is added. The OPF is then performed corresponding to PV and wind power sources addition and saves the right solution in each situation. The independent control parameter is the active power taken from the generator and the HOA as represented in Eq. (5) holds it within its borders. The limits of the equalities represented in Eq. (3), (4), and (6) are fulfilled with the use of MAT-POWER toolbox [32] and the MATLAB environment with the Newton-Raphson power flow. The inclusion of penalty factors is to satisfy the objective without constraint violations, limits the other dependent variables. These penalties are represented mathematically in Eq. (9) [9].

$$Penalties = K_v \sum_{i=1}^{N} \left[ \max\left(0, V_i - V_i^{max}\right) + \max\left(0, V_i^{min} - V_i\right) \right] + K_l \sum_{j=1}^{nbr} \left[ \max\left(0, S_j - S_j^{rated}\right) \right] \quad (9)$$

where $K_v$ and $K_l$ are great positive numbers.

## III. THE HOA

In organizations, the employees are grouped under a hierarchy that can be named CRH, a form of social contact among people can be seen. This rises the administrative structures such that people can accomplish the corporate objectives effectively. A treelike arrangement is the hierarchy of businesses. The supervisor is assigned to the highest level and the workers are assigned to the parent-child nodes. Subordinates are responsible for communicating their immediate supervisor. People on the same stage are the colleagues.

### A. INSPIRATION

The framework of the organization is a collection of strategies that organize the task. This system has aimed at arranging the tasks and meeting the final aims in an optimum way.

The definition is divided into four steps:
- CRH modeling,
- Modeling the relationship between assistants and the head,
- Modeling the relationship between the colleagues,
- Modeling an employee self-contribute to a job.

### B. MODELING THE CRH

Given the existence of CRH, the Heap Data Structure is used as a basis for CRH. The entire CRH is the population. A search agent is the heap node during the deployment process. The key to the node in this heap is the fitness of the population and the search agent index in the population is known to be the heap node. A heap data structure of the method of CRH modelling is more illustrated in Fig. 2 [24].



(a)  Search space

(b)  Objective space

(c)  Heapify the population
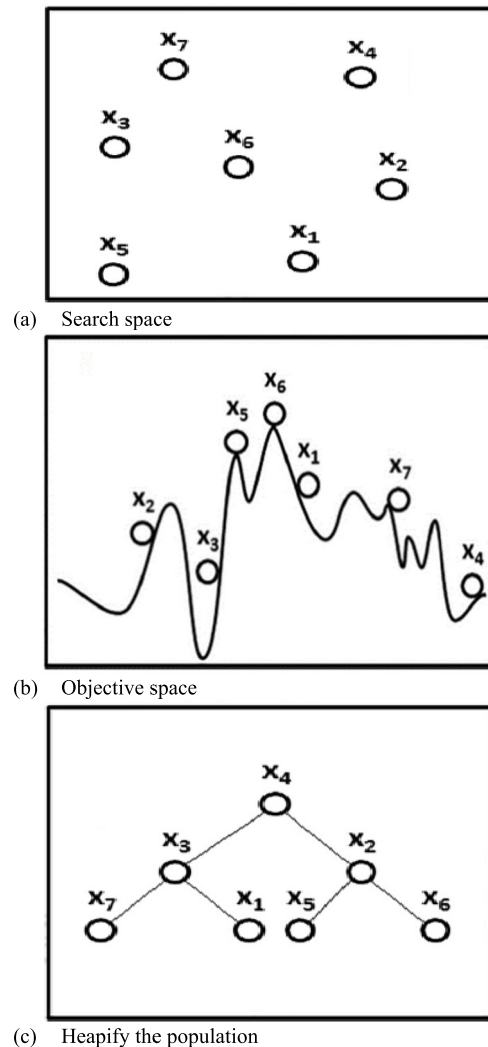
**FIGURE 2.** Modeling of the CRH with min-heap, (a) Search space, (b) Objective space, (c) Heapify the population.

### C. MODELING OF THE COLLABORATION WITH THE BOSS

Regulations are implemented in a structured hierarchical system of the highest ranks and subordinates obey their supervisor. This action is modeled, by modifying the location of the candidate $\vec{x}_i$ with regard to the parent node B, by eq. (10). Each parent node is a supervisor for its children [24]:

$$x^i(t+1) = B^k + \gamma \lambda^k |B^k - x_i(t)| \quad (10)$$

where $t$ is the ongoing iteration, $k$ is the $k$th component of a vector. $\lambda^k$ represents the $k$th component of vector $\vec{\lambda}$. It's calculated as in eq. (11) [24]:

$$\lambda^k = 2r - 1 \quad (11)$$

where $r$ is random number between [0], [1]. $\lambda$ is calculated as in eq. (12) [24]:

$$\gamma = \left| 2 - \frac{\left(t \bmod \frac{T}{C}\right)}{\frac{T}{4C}} \right| \quad (12)$$
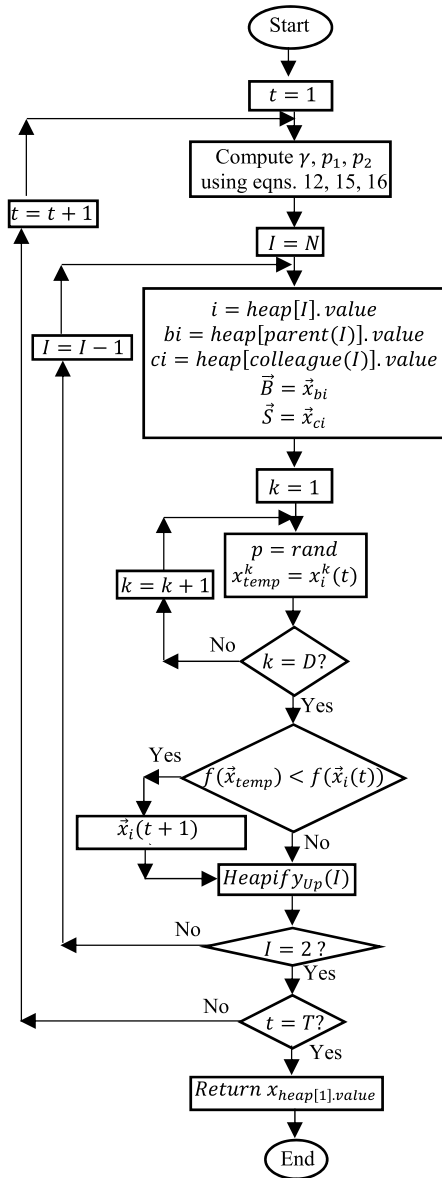
**FIGURE 3. Flow chart of the HOA algorithm.**

where $T$ is the maximum iterations. $C$ is a parameter that determines the number of cycles $\gamma$ in $T$ iterations. Through the iterations, $\gamma$ decreases linearly from 2 to 0. After it equals 0, it increases again to 2.

### D. MODELING OF THE COLLABORATION BETWEEN COLLEAGUES

The colleagues collaborate and execute the official duties. In a heap, the same level nodes are colleagues. Accordingly, a population $\vec{x}_i$ modifies its position with respect to a colleague $\vec{S}_r$. This is represented in eq. (13) [24]:

$$x_i^k (t+1) = \begin{cases} S_r^k + \gamma \lambda^k \left| S_r^k - x_i^k (t) \right|, & f\left(\vec{S}_r\right) < f\left(\vec{x}_i(t)\right) \\ x_i^k + \gamma \lambda^k \left| S_r^k - x_i^k (t) \right|, & f(\vec{S}_r) \geq f\left(\vec{x}_i(t)\right) \end{cases}$$
(13)

where $f$ is the fitness function. The randomness in colleagues' selection integrates the search around fit candidates, which enhances the exploitation process.

### E. MODELING OF AN EMPLOYEE SELF-CONTRIBUTION

This process simulates an employee self-impact. It is charted simply with some variants suggestions. It is modelled by maintaining the employee's former position into the upcoming iteration, as expressed in eq. (14) [24]:

$$x_i^k (t+1) = x_i^k (t)$$
(14)

The population $\vec{x}_i$ keeps its position for the $k$th control variable for the upcoming iteration.

### F. PUTTING ALL TOGETHER

The challenge is to determine the selection probabilities for the three equations to balance exploration and exploitation processes. A roulette wheel is intended to balance the probabilities. It is divided into three parts $p_1$, $p_2$, and $p_3$. The selection of $p_1$ makes a population to modify the position. The $p_1$ is limited by eq. (15) [24]:

$$p_1 = 1 - \frac{t}{T}$$
(15)

The $p_2$ is limited by eq. (16):

$$p_2 = p_1 + \frac{1 - p_1}{2}$$
(16)

Finally, $p_3$ is computed as in eq. (17):

$$p_3 = p_2 + \frac{1 - p_1}{2} = 1$$
(17)

The updating mechanism of the HOA is expressed in eq. (18) [24]:

$$x_i^k (t+1)$$

$$= \begin{cases} x_i^k (t), p \leq p_1 \\ B^k + \gamma \lambda^k \left| B^k - x_i^k (t) \right|, \\ \quad p > p_1 \text{ and } p \leq p_2 \\ S_r^k + \gamma \lambda^k \left| S_r^k - x_i^k (t) \right|, \\ \quad p > p_2 \text{ and } p \leq p_3 \text{ and } f\left(\vec{S}_r\right) < f\left(\vec{x}_i(t)\right) \\ x_i^k + \gamma \lambda^k \left| S_r^k - x_i^k (t) \right|, \\ \quad p > p_2 \text{ and } p \leq p_3 \text{ and } f(\vec{S}_r) \geq f\left(\vec{x}_i(t)\right) \end{cases}$$
(18)

where $p$ is a number between [0], [1].

### G. IMPLEMENTATION OF THE HOA

The time and complexity of the introduced method are not influenced by using the heap into the implementation of HOA. The flow chart of the proposed HOA optimization method is shown in Fig. 3.

where $i$ is the index the population P of the $I^{th}$ node. $bi$ and $ci$ are the parent and colleague indices, respectively. $\vec{B}$ and $\vec{S}$ are the parent and colleague position vectors, respectively.

**TABLE 1.** Key features of the three studied systems.

| Number of | IEEE 30 | IEEE 57 | IEEE 118 |
|---|---|---|---|
| buses | 30 | 57 | 118 |
| generators | 6 | 7 | 54 |
| branches | 41 | 80 | 186 |
| transformers | 4 | 17 | 9 |
| loads | 21 | 42 | 99 |
| connected loads (MVA) | 283.4+j126.2 | 1250+j336.4 | 4242+j1438 |
| Load losses (MVA) | 5.28+j23.14 | 16+j72.97 | 132.86+j783.79 |

**TABLE 2.** Simulation parameters of HOA and GA.

| | | IEEE test system | | |
|---|---|---|---|---|
| | | 30-bus | 57-bus | 118-bus |
| | HOA | 348.3 | 381.5 | 1880.4 |
| | GA | 528.6 | 11002 | 4006.3 |
| Simulation Time (s) | PSO | 332.3 | 125.93 | - |
| | MPA | 299.1043 | 763.11663 | - |
| | HHO | - | 2095.25 | 14717.87 |

**TABLE 3.** Optimal fitness and population values for the base case OPF for system 1.

| Generator power (MW) at bus | HOA | GA | PSO [9] | MPA |
|---|---|---|---|---|
| 1 | 227.5524643 | 205.8909 | 197.89 | 197.253246 |
| 2 | 20 | 27.36848 | 49.98 | 44.8174083 |
| 13 | 16.65898938 | 18.92830 | 15 | 20.3995709 |
| 22 | 10 | 14.46586 | 10 | 10.0155727 |
| 23 | 10 | 12.85073 | 10.015 | 10 |
| 27 | 12 | 15.04132 | 12 | 12 |
| Min cost($/hr) | 906.38723695 | 914.0514 | 917.93 | 915.78184 |

1) STEPS OF THE PROPOSED HOA

1) Parameters Definition.
2) Population Initialization.
3) Heap building (parent, child, depth, colleague, and Heapify_Up).
4) The heap key and value save the fitness and the population that corresponds the fitness, respectively.

Populations modify the locations to converge on the best solution.

## IV. DISCUSSION ON THE SIMULATION RESULTS

This paper introduces the OPF solved using the proposed HOA. To analyse the validity of the proposed HOA-based OPF, the standard IEEE 30-, 57- and 118- bus networks are used. Table 1 presents the key characteristics of the three systems under study. Systems 1, 2, and 3 stands for the IEEE 30-, 57- and 118-bus test systems, respectively.

**TABLE 4.** Optimal fitness and population values for the base case OPF for system 2.

| Generator power (MW) at bus | HOA | GA | PSO [9] | HHO [13] | MPA |
|---|---|---|---|---|---|
| 1 | 144.8560492 | 151.43944 | 153.41 | 144.89 | 144.856 |
| 2 | 93.0378376 | 85.655155 | 0 | 94.85 | 93.0378 |
| 3 | 45.2090453 | 47.316627 | 47.07 | 45.08 | 45.209 |
| 6 | 68.26235865 | 63.81441 | 61.09 | 65.9 | 68.26235 |
| 8 | 457.026782 | 471.12909 | 550 | 457.17 | 457.0267 |
| 9 | 95.8565251 | 75.268325 | 89.58 | 96.009 | 95.8565 |
| 12 | 365.956972 | 375.58131 | 374.31 | 366.24 | 365.95697 |
| Min cost($/hr) | 41872.903 23 | 41891.3 742 | 42262. 61 | 41873.0 6 | 41872.9 903 |

The design variables of the OPF are the active output power from the generators. The objective is targeted sequentially as explained in the upcoming sections:
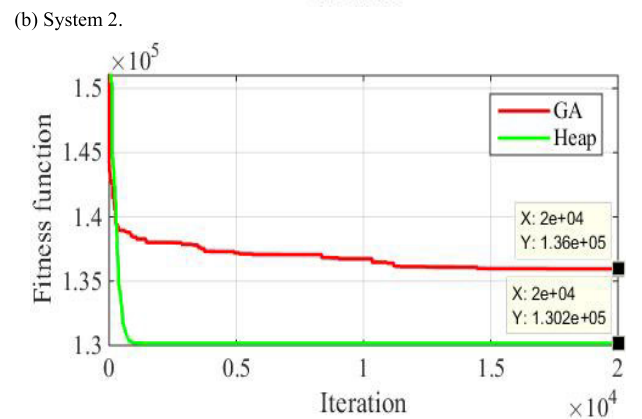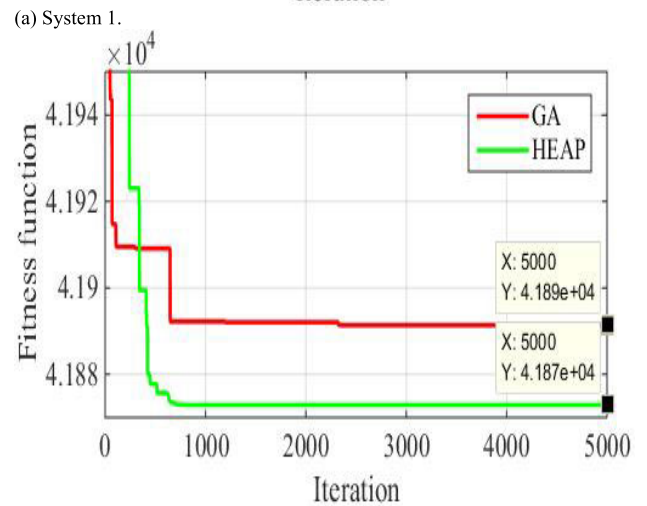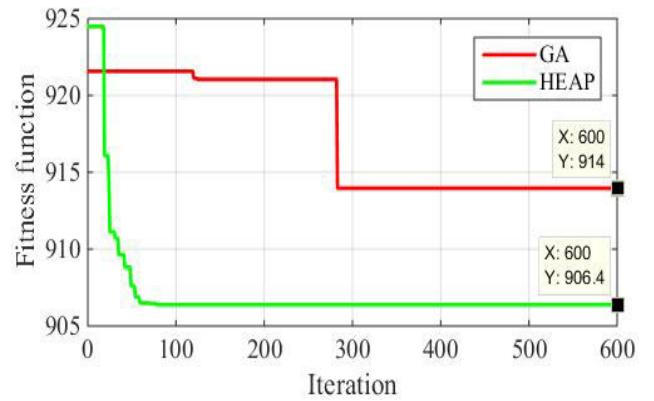
### A. OPF (THE BASE CASE)

The meant by the base case is the case without insertion of any green energy sources, the OPF is performed on the standard IEEE 30-, 57-, 118- bus test networks. The maximum and minimum boundaries of the control variables of the three systems under study are found in [32]. The number of iterations is chosen to be the stopping criteria of the simulation and the point of the comparison between the HOA and GA. In the IEEE 30-, 57-, 118-bus systems, the maximum numbers of iterations are 600, 5000, 20000, respectively. The objective is the fuel cost minimization. For the three systems studied and all scenarios, the values of the bus voltage and the line flow penalty factors are $9 \times 10^{15}$ and $9 \times 10^{13}$, respectively. A relation between the proposed HOA and GA with respect to the simulation time is seen in Table 2. It can be noted that the HOA needs much lower time than the GA to finish the simulation process. Further data of the dependent variables (Transmission Line apparent power and the Generator reactive power) is attached at the end of this paper after the conclusion section.

For more detailed results, Tables 3-5 are presented to obtain the control variables that correspond the optimal values of the fitness function for the three standard test systems, the IEEE 30-, 57-, and 11-bus test systems, respectively. The figures of the convergence curves of the fitness function are provided with the three test systems. In Fig. 4 a-c, the comparisons between the performance of the HOA and GA convergence of the three studied systems are shown. The general remark for the simulations of the whole systems is that the fitness function converged fast and smoothly in the case of using the new proposed algorithm. For the base OPF case,

**TABLE 5.** Optimal fitness and population values for the base case OPF for system 3.

| Generator power (MW) at bus | HOA | GA | HHO [13] |
|---|---|---|---|
| 1 | 25.9569064448638 | 46.64348288 | 6.14 |
| 4 | 0 | 32.60295454 | 0.02 |
| 6 | 2.79295179374116 | 38.08212633 | 9.47 |
| 8 | 0 | 26.19771312 | 29.64 |
| 10 | 401.153508538168 | 272.3710272 | 418.52 |
| 12 | 86.4024929847601 | 73.22827184 | 81.38 |
| 15 | 23.7553765283501 | 38.00522085 | 1.53 |
| 18 | 15.5321497214307 | 34.73950011 | 41.21 |
| 19 | 22.5286788592375 | 40.75631948 | 5.35 |
| 24 | 0 | 45.96633966 | 0.89 |
| 25 | 194.038964055319 | 131.1105628 | 205.95 |
| 26 | 279.900508903909 | 217.7297736 | 286.68 |
| 27 | 15.5852003642891 | 31.14068180 | 1.2 |
| 31 | 7.33295615709312 | 23.00674347 | 7.28 |
| 32 | 0 | 50.91634097 | 13.63 |
| 34 | 7.45998354223770 | 30.65930124 | 9.47 |
| 36 | 12.9586665902067 | 42.57814840 | 4.02 |
| 40 | 51.9899982657949 | 36.82208311 | 13.46 |
| 42 | 45.5877409328148 | 42.65108000 | 17.48 |
| 46 | 19.1512252820705 | 31.82180145 | 16.89 |
| 49 | 194.368094547667 | 125.4309740 | 201.58 |
| 54 | 49.5997668701826 | 52.65948198 | 52.46 |
| 55 | 32.5979296835137 | 41.29486450 | 12.001 |
| 56 | 33.3989030918837 | 51.30437655 | 33.6 |
| 59 | 149.965921221199 | 111.2667226 | 155.42 |
| 61 | 148.357681279316 | 113.5439380 | 156.8 |
| 62 | 0 | 50.44757113 | 1.63E-05 |
| 65 | 352.842910139785 | 288.9085804 | 354.2 |
| 66 | 350.053226789271 | 229.0812981 | 351.75 |
| 69 | 454.548251958255 | 314.3999459 | 458.96 |
| 70 | 0 | 45.36362440 | 38.86 |
| 72 | 0 | 40.87926448 | 1.61E-05 |
| 73 | 3.9071177433e-11 | 42.24423377 | 4.62 |
| 74 | 16.1400267200474 | 55.42070675 | 9.96 |
| 76 | 19.1941898860551 | 40.80981321 | 5.31 |
| 77 | 0 | 43.01983463 | 39.73 |
| 80 | 432.577039496406 | 276.9136770 | 373.61 |
| 85 | 0 | 39.54586246 | 6.01E-06 |
| 87 | 3.62153149115355 | 13.28940124 | 3.54 |
| 89 | 495.596247101245 | 328.0306755 | 506.89 |
| 90 | 0 | 41.98526830 | 5.70E-07 |
| 91 | 0 | 48.71205557 | 4.05 |
| 92 | 3.0472483391e-13 | 45.01746368 | 2.11E-05 |
| 99 | 0 | 45.43678927 | 29.26 |
| 100 | 231.381382531255 | 157.5240341 | 232.49 |
| 103 | 38.3907670990906 | 35.41607758 | 37.89 |
| 104 | 8.2367412732e-12 | 42.73532186 | 6.49 |
| 105 | 4.37502795687037 | 38.51249849 | 2.82 |
| 107 | 29.4981684339238 | 40.73271291 | 22.52 |
| 110 | 6.67915923130552 | 38.59811299 | 30.76 |
| 111 | 35.0740731619637 | 44.21429573 | 31.5 |
| 112 | 40.8927288763138 | 47.27614646 | 10.07 |
| 113 | 0 | 41.84418476 | 3.75 |
| 116 | 2.7195183515e-12 | 47.72560846 | 7.61E-06 |
| Min cost($/hr) | 130160.197435109 | 135957.3447 | 130599.75 |



(a) System 1.



(b) System 2.



(c) System 3.

**FIGURE 4.** Convergence of the objective function for: (a) System 1, (b) System 2, (c) System 3.

**TABLE 6.** Optimal locations for PV and wind energy sources.

| Test system | 30-bus | 57-bus | 118-bus |
|---|---|---|---|
| Optimal PV location | 4 | 47 | 114 |
| Optimal wind farm location | 21 | 48 | 15 |

the percentage reductions in the fuel cost of the 30-, 57-, 118-bus systems obtained due to the employment of the HOA by solving the OPF are 0.8%, 0.04%, and 4.26 %, respectively. It is observed that the HOA performs better when the system becomes larger.
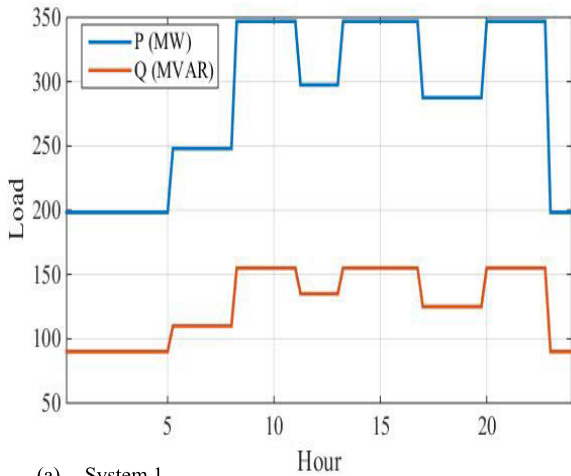
## B. OPTIMAL ALLOCATION OF PV PANEL AND WIND FARM
The second stage of this research is to find an optimal bus at which a PV panel can be placed and the same for a

(a) System 1.
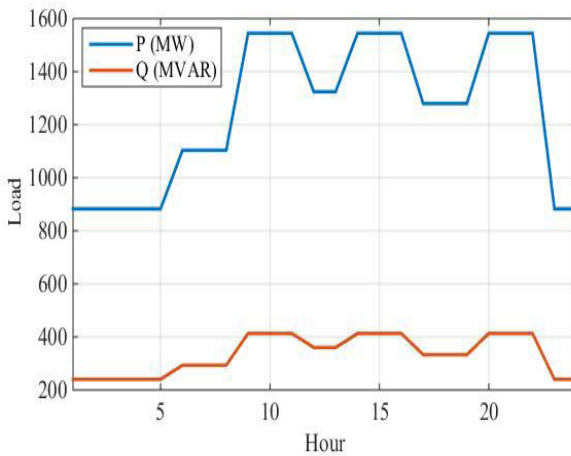


(b) System 2.



(c) System 3.

**FIGURE 5.** Load Curves of the IEEE test systems, (a) System 1, (b) System 2, (c) System 3.

**TABLE 7.** Scenarios of OPF.

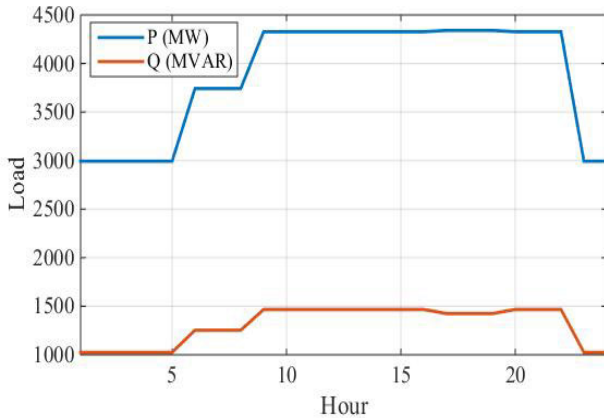| Scenario No. | Test system | PV panel at bus | Wind farm at bus |
|---|---|---|---|
| 1 | 30-bus system | - | - |
| | 57-bus system | - | - |
| | 118-bus system | - | - |
| 2 | 30-bus system | 4 | - |
| | 57-bus system | 47 | - |
| | 118-bus system | 114 | - |
| 3 | 30-bus system | - | 21 |
| | 57-bus system | - | 48 |
| | 118-bus system | - | 15 |
| 4 | 30-bus system | 4 | 21 |
| | 57-bus system | 47 | 48 |
| | 118-bus system | 114 | 15 |

**TABLE 8.** Simulation time taken by the HOA in the four studied scenarios.

| Test System | Scenario | Simulation time (s) | |
|---|---|---|---|
| | | HOA | GA |
| IEEE 30-bus | None | 2723.75 | 1656.4 |
| | PV | 2167.03 | 2209.975 |
| | Wind | 1162.48 | 1518.71 |
| | Hybrid | 1817.68 | 2232.21 |
| IEEE 57-bus | None | 2028.19 | 2958.869 |
| | PV | 1446.36 | 2319.9102 |
| | Wind | 1800.79 | 2605.3106 |
| | Hybrid | 2304.13 | 2578.7148 |
| IEEE 118-bus | None | 1840.2 | 2506.93035 |
| | PV | 3205.57 | 4666.767 |
| | Wind | 6862.8 | 4697.514 |
| | Hybrid | 3921.12 | 4739.019 |

**TABLE 9.** Reactive power of the generators:30-bus system.

| Generator Number | Generator at bus | Generator reactive power |
|---|---|---|
| 1 | 1 | -15.75247491 |
| 2 | 2 | 51.94564166 |
| 3 | 5 | 27.92964763 |
| 4 | 8 | 26.85483047 |
| 5 | 11 | 15.37332392 |
| 6 | 13 | 8.594153394 |

wind turbine. The optimal bus is the bus that corresponds to a minimum fuel cost when performing the OPF problem considering insertion of the PV panels at the whole buses one at a time. This is studied for the three aforementioned IEEE bus test systems, 30-bus, 57-bus, and 118-bus systems. The SFO algorithm is employed for this task in case of the IEEE 30-bus system. Meanwhile, the HHO algorithm is the one which is employed for this task in case of the IEEE 57-bus system and the 118-bus system. The optimal bus for a PV panel only is targeted first. Then, the optimal bus for a wind farm only is targeted. Table 6 presents the results of the simulations of this stage, which is the optimal locations for the PV panel and the wind farm in the case of each test system. These locations are used in the OPF with renewable energy sources (RES) and variable loading conditions which is the next stage of the research and they are presented in detail in the following section. The PV and wind energy sources are considered stepped negative loads and the uncertainty is neglected in this study for simplicity [33]–[36].

**TABLE 10.** Reactive power of the generators: 57-bus system.

| Generator Number | Generator at bus | Generator reactive power |
|---|---|---|
| 1 | 1 | 190.271881 |
| 2 | 2 | -28.70704164 |
| 3 | 3 | -6.198962902 |
| 4 | 6 | -21.68044383 |
| 5 | 8 | 61.03808859 |
| 6 | 9 | -19.26355139 |
| 7 | 12 | 108.1101916 |

## C. OPF WITH RES PENETRATION AND VARIABLE LOADING CONDITIONS

In the final stage of the study, the OPF single objective optimization problem is targeted with various scenarios and loading conditions. These scenarios represent the integration of the PV panel only, the wind farm only, both PV panel and the wind farm with the systems under study. The loading conditions are not constant over the day, but they change their values hourly. All scenarios and loading variation are tested for the three systems, 30-bus, 57-bus, and 118-bus systems. The order of performing the OPF scenarios is as follows: (1) The OPF is performed firstly without insertion of PV panels or wind farms, only the load is changing hourly. (2) The OPF is performed with only PV panel is added to the previously determined optimal bus for the whole test systems. (3) The OPF is performed with only wind farm is added to the previously selected optimal bus for each test system. (4) The last scenario is to perform the OPF with including PV panel and wind farm in addition to the hourly changing loads for the three test systems. The summary of these scenarios is presented in Table 7. The comparisons for all scenarios are presented between the newly proposed HOA and the well-established GA. The load curves of the systems under study are shown in Fig. 5 a-c.

In scenario 1, The results obtained by the newly developed HOA and GA are close together in the 30-bus system, but the HOA obtained better results in the 57-bus and the 118-bus systems, especially during the hours of high loading condition. The HOA results present a percentage reduction of 1.018% compared with the GA results when testing the 30-bus system. The percentages of reduction are about 0.7% and 9% of the 57- bus and 118- bus systems, respectively. The hourly comparisons between the HOA and GA in the fuel cost of the three test systems are shown in Fig. 6 a-c.

In scenario 2, the PV panel is added to bus 4 in the 30-bus system, while it is added to bus 47 in the 57-bus system, and it is added to bus 114 in the 118-bus system. The HOA resulted in a percentage reduction of 1.015% compared with the GA results when testing the 30-bus system. The percentages of reduction are about 3.3% and 6.2% of the 57- bus



(a) System 1.
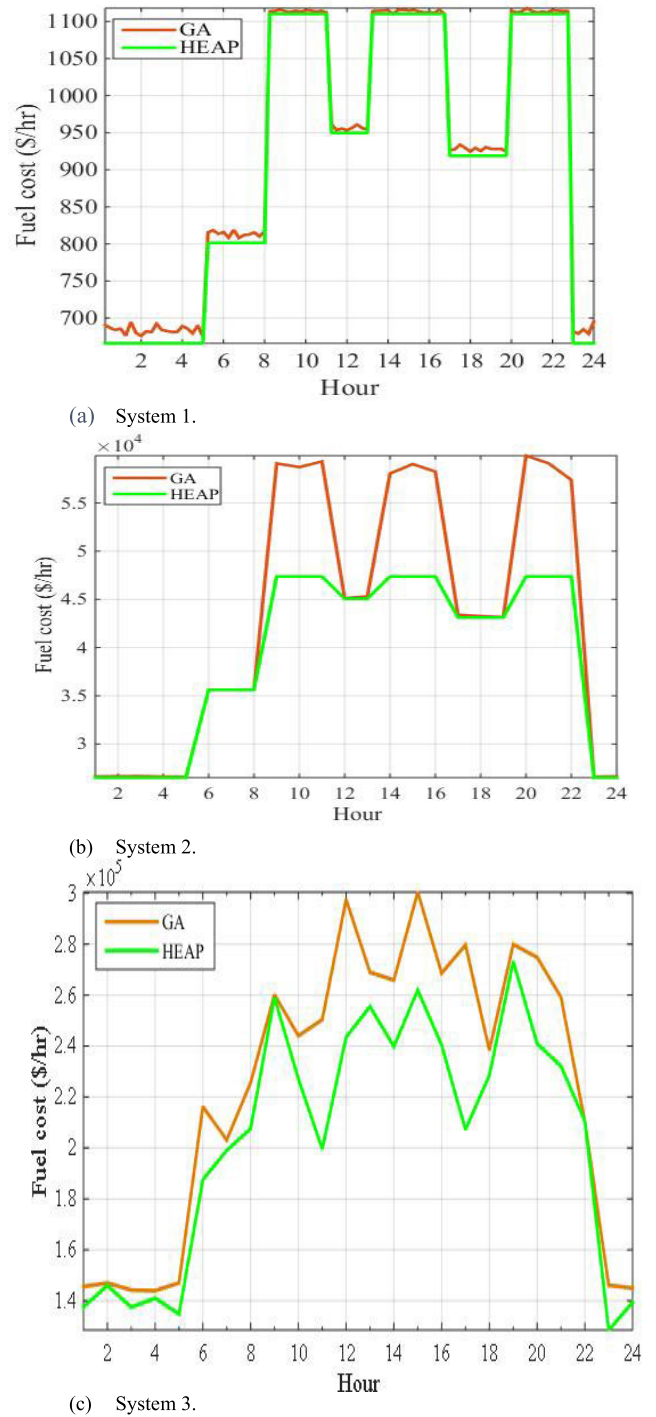
(b) System 2.

(c) System 3.

**FIGURE 6.** Scenario 1 results for (a) System 1, (b) System 2, (c) System 3.

and 118- bus systems, respectively. The hourly comparisons between the HOA and GA of the fuel cost of the three test systems are shown in Fig. 7 a-c.

In scenario 3, the wind farm is added to bus 21 in the 30-bus system, while it is added to bus 48 in the 57-bus system, and it is added to bus 15 in the 118-bus system. The HOA resulted in a percentage reduction of 1.33% compared with the GA results when testing the 30-bus system. The percentages of
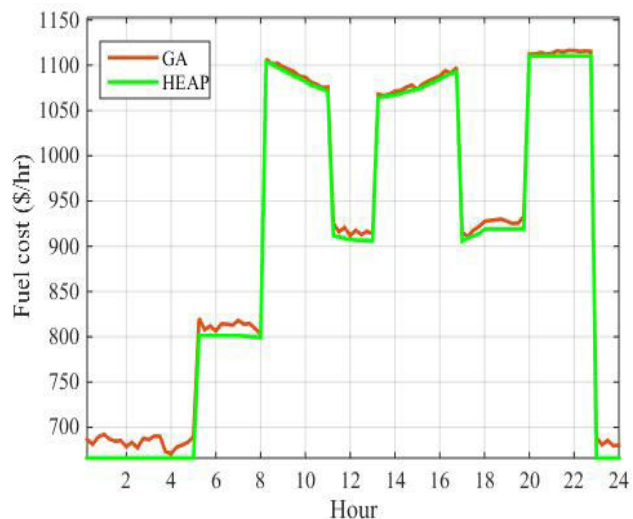
(a)　System 1.
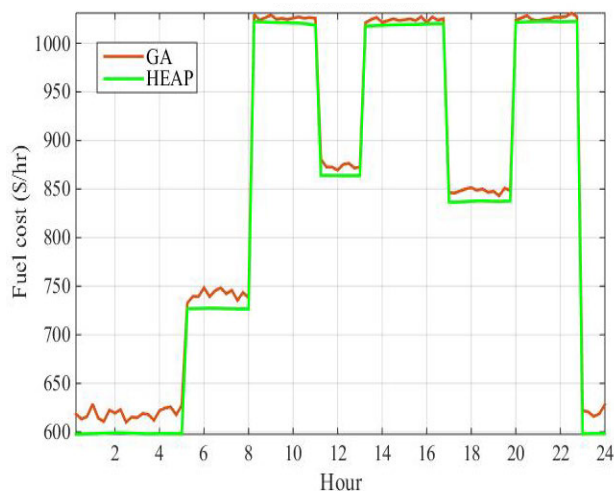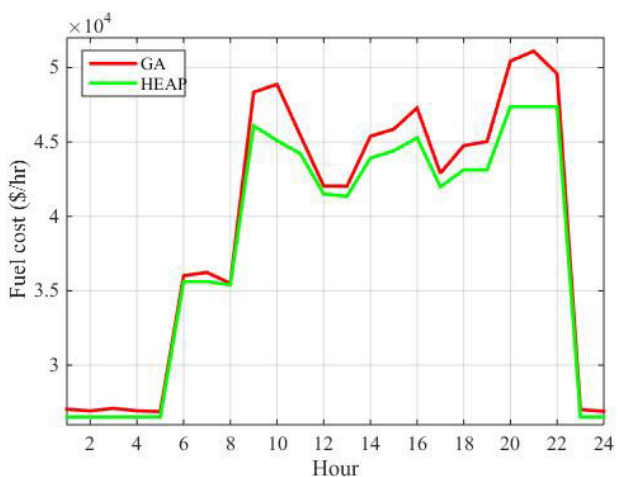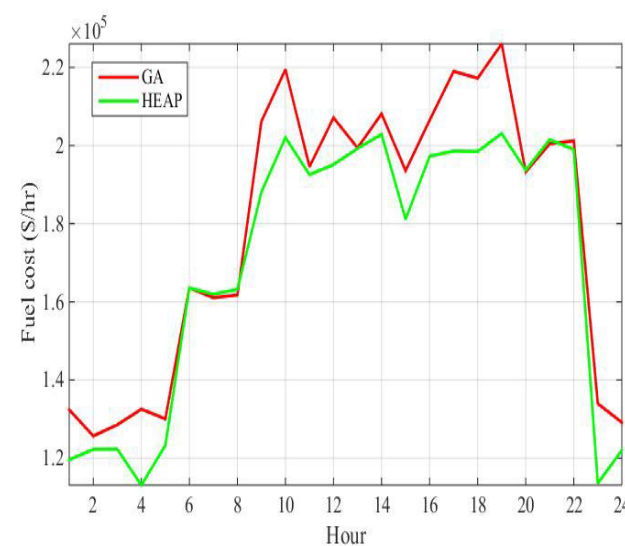


(b)　System 2.



(c)　System 3.

**FIGURE 7.** Scenario 2 results for, (a) System 1, (b) System 2, (c) System 3.



(a)　System 1.



(b)　System 2.



(c)　System 3.

**FIGURE 8.** Scenario 3 results for, (a) System 1, (b) System 2, (c) System 3.
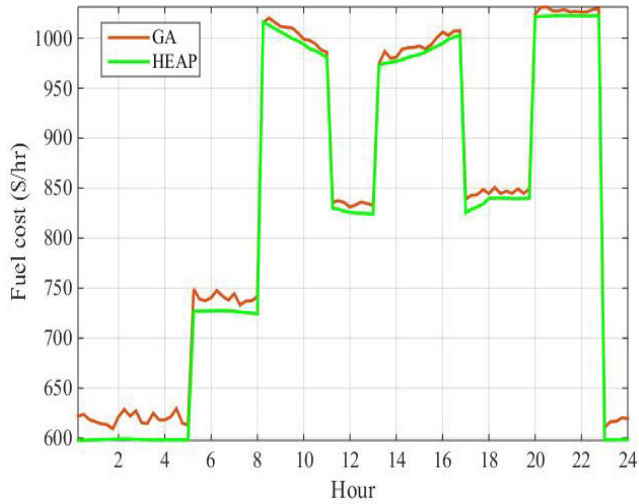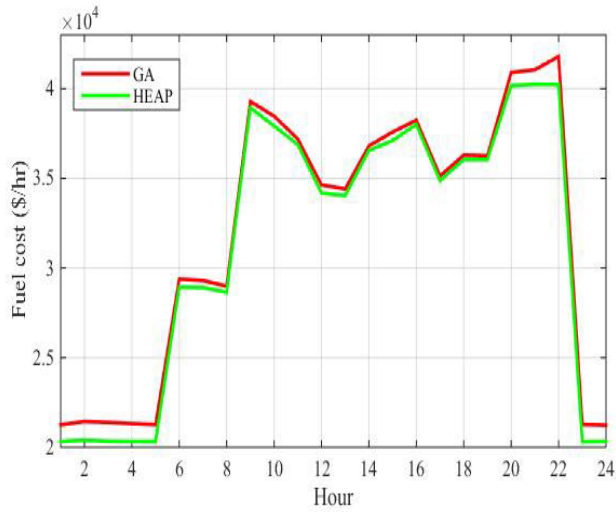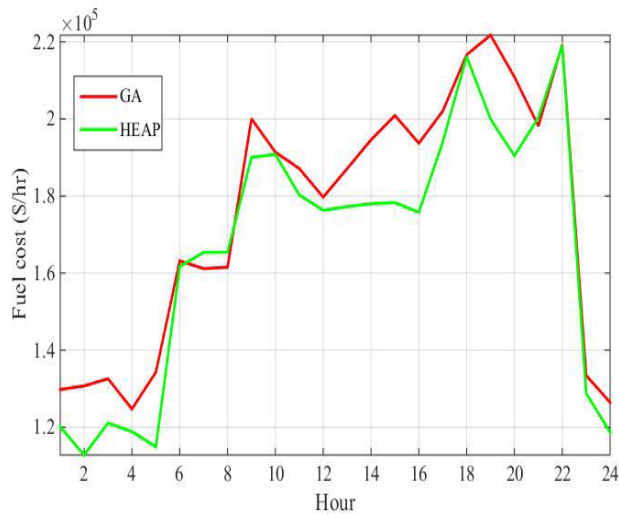
(a)    System 1.



(b)    System 2.



(c)    System 3.

**FIGURE 9.** Scenario 4 results for, (a) System 1, (b) System 2, (c) System 3.

**TABLE 11.** Reactive power of the generators:118-bus system.

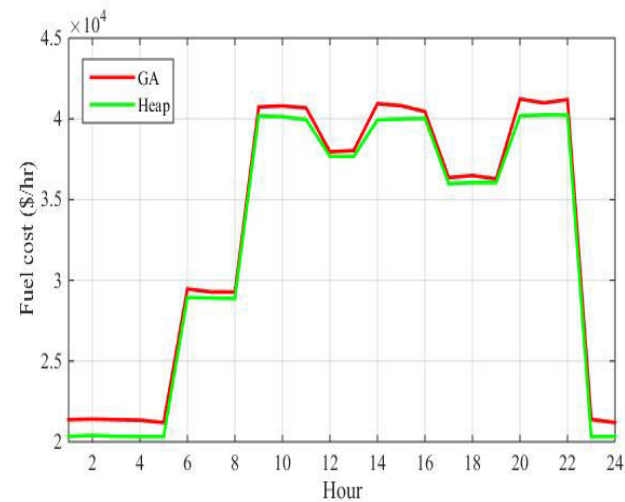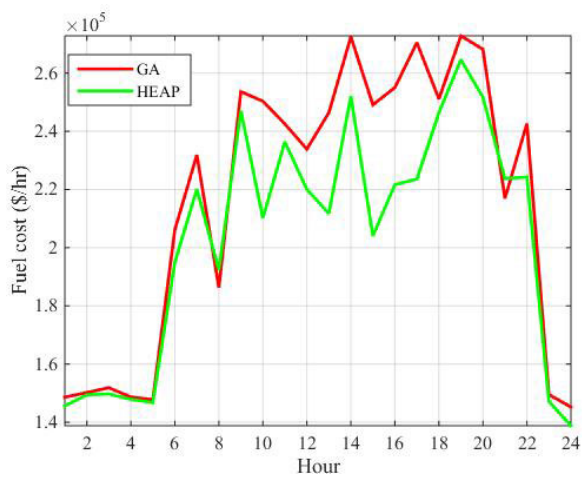| Generator Number | Generator at bus | Generator reactive power |
|---|---|---|
| 1 | 1 | -11.2476704 |
| 2 | 4 | -12.45792307 |
| 3 | 6 | 15.28730561 |
| 4 | 8 | 39.85669482 |
| 5 | 10 | -59.23663371 |
| 6 | 12 | 90.2374437 |
| 7 | 15 | -1.672212604 |
| 8 | 18 | 23.27792099 |
| 9 | 19 | -21.24316881 |
| 10 | 24 | -14.92947761 |
| 11 | 25 | 49.31223299 |
| 12 | 26 | 4.057031498 |
| 13 | 27 | -2.637959913 |
| 14 | 31 | 32.34997513 |
| 15 | 32 | -18.48815206 |
| 16 | 34 | -23.82700753 |
| 17 | 36 | 3.757068701 |
| 18 | 40 | 8.7382155 |
| 19 | 42 | 21.62167896 |
| 20 | 46 | -7.224990196 |
| 21 | 49 | 97.68177363 |
| 22 | 54 | 2.107681508 |
| 23 | 55 | -4.948186924 |
| 24 | 56 | -15.27853212 |
| 25 | 59 | 77.78394618 |
| 26 | 61 | -40.67549821 |
| 27 | 62 | 0.994742494 |
| 28 | 65 | 68.1430576 |
| 29 | 66 | 3.577486473 |
| 30 | 69 | -78.25962196 |
| 31 | 70 | 5.983671988 |
| 32 | 72 | -11.1768749 |
| 33 | 73 | 9.599729279 |
| 34 | 74 | -11.96799702 |
| 35 | 76 | -2.282364886 |
| 36 | 77 | 7.695871815 |
| 37 | 80 | 107.1652732 |
| 38 | 85 | -6.970082711 |
| 39 | 87 | 11.09654834 |
| 40 | 89 | 5.172437875 |
| 41 | 90 | 58.74559434 |

**TABLE 11.** *(Continued.)* Reactive power of the generators:118-bus system.

| | | |
|---|---|---|
| 42 | 91 | -12.87985349 |
| 43 | 92 | -24.65757799 |
| 44 | 99 | -17.53594418 |
| 45 | 100 | 90.92458963 |
| 46 | 103 | 67.14758811 |
| 47 | 104 | 0.603183536 |
| 48 | 105 | -21.68808174 |
| 49 | 107 | -3.574086159 |
| 50 | 110 | -1.510603936 |
| 51 | 111 | -1.602239182 |
| 52 | 112 | 23.91705664 |
| 53 | 113 | 5.866585957 |
| 54 | 116 | 53.43720708 |

reduction are 2.13% and 4.8% of the 57- bus and 118- bus systems, respectively. The hourly comparisons between the HOA and GA of the fuel cost of the three test systems are shown in Fig. 8 a-c.

In scenario 4, PV panel is added to bus 4 and the wind farm is added to bus 21 in the 30-bus system, while they are added to buses 47 and 48 respectively in the 57-bus system, and they are added to buses 114, and 15 respectively in the 118-bus system. The HOA resulted in a percentage reduction of 1.36% compared with GA when testing the 30-bus system. The percentages of reduction are 1.94% and 4.85% of the 57- bus and 118- bus systems, respectively. The hourly comparisons between the HOA and GA of the fuel cost of the three test systems are shown in Fig. 9 a-c. The simulation times taken by the proposed HOA and the GA algorithms for the studied scenarios are summarized in Table 8.

From the results, it can be observed that using the proposed algorithm led to improvement in results of the objective function in the base case of the OPF problem by (0.84 – 1.227) % for the first test system, (0.00038 – 0.93) % for the second test system, (0.33 – 4.45) % for the third test system. On the other hand, when comparing the simulation time, it can be seen that the HOA is the fastest in the third test system, but it came second in speed after the PSO in the first and second test systems.

For further considerations and future works, energy storage is now included in Active Network Management schemes. Dynamic optimal power flow is an extension of OPF to cover multiple time periods [37]. Moreover, demand response (DR) represents an important part of the electrical power network operation. Also, Smart grids will increase the utilization of DR [37]. DR is also implemented for planning decisions [39]. On the other hand, In [40], planning for optimal allocation

**TABLE 12.** Transmission Line apparent power:30-bus system.

| Transmission Line Number | From bus | To bus | Apparent Power |
|---|---|---|---|
| 1 | 1 | 2 | 155.4198749 |
| 2 | 1 | 3 | 73.57224631 |
| 3 | 2 | 4 | 34.07814149 |
| 4 | 3 | 4 | 68.85524635 |
| 5 | 2 | 5 | 67.34270628 |
| 6 | 2 | 6 | 47.53216733 |
| 7 | 4 | 6 | 60.4182131 |
| 8 | 5 | 7 | 16.63567629 |
| 9 | 6 | 7 | 35.55840523 |
| 10 | 6 | 8 | 20.64984534 |
| 11 | 6 | 9 | 21.59323169 |
| 12 | 6 | 10 | 13.21721146 |
| 13 | 9 | 11 | 18.33954984 |
| 14 | 9 | 10 | 30.20966238 |
| 15 | 4 | 12 | 36.84249125 |
| 16 | 12 | 13 | 14.76006343 |
| 17 | 12 | 14 | 8.401172873 |
| 18 | 12 | 15 | 19.91648543 |
| 19 | 12 | 16 | 8.546427953 |
| 20 | 14 | 15 | 1.882263273 |
| 21 | 16 | 17 | 4.566905777 |
| 22 | 15 | 18 | 6.570520155 |
| 23 | 18 | 19 | 3.193977124 |
| 24 | 19 | 20 | 7.004546139 |
| 25 | 10 | 20 | 9.437584732 |
| 26 | 10 | 17 | 6.634091765 |
| 27 | 10 | 21 | 18.82773198 |
| 28 | 10 | 22 | 8.990034159 |
| 29 | 21 | 22 | 2.225750053 |
| 30 | 15 | 23 | 6.349604968 |
| 31 | 22 | 24 | 6.759873069 |
| 32 | 23 | 24 | 2.70993001 |
| 33 | 24 | 25 | 1.600921465 |
| 34 | 25 | 26 | 4.261951421 |
| 35 | 25 | 27 | 3.775790927 |
| 36 | 28 | 27 | 17.77549593 |
| 37 | 27 | 29 | 6.410727057 |
| 38 | 27 | 30 | 7.284049848 |
| 39 | 29 | 30 | 3.752880066 |
| 40 | 8 | 28 | 2.638686901 |
| 41 | 6 | 28 | 16.60363158 |

**TABLE 13.** Transmission Line apparent power:57-bus system.

| Transmission Line Number | From bus | To bus | Apparent Power |
|---|---|---|---|
| 1 | 1 | 2 | 136.8739806 |
| 2 | 2 | 3 | 45.00941586 |
| 3 | 3 | 4 | 16.48842256 |
| 4 | 4 | 5 | 14.71053677 |
| 5 | 4 | 6 | 24.92938294 |
| 6 | 6 | 7 | 14.11724613 |
| 7 | 6 | 8 | 42.08345953 |
| 8 | 8 | 9 | 185.0274771 |
| 9 | 9 | 10 | 38.82630026 |
| 10 | 9 | 11 | 45.89516423 |
| 11 | 9 | 12 | 27.67684097 |
| 12 | 9 | 13 | 35.60560815 |
| 13 | 13 | 14 | 22.73172213 |
| 14 | 13 | 15 | 15.44930954 |
| 15 | 1 | 15 | 72.3662944 |
| 16 | 1 | 16 | 34.92059111 |
| 17 | 1 | 17 | 49.45379966 |
| 18 | 3 | 15 | 52.93824921 |
| 19 | 4 | 18 | 14.23545414 |
| 20 | 4 | 18 | 17.9930532 |
| 21 | 5 | 6 | 25.35035905 |
| 22 | 7 | 8 | 82.5351172 |
| 23 | 10 | 12 | 23.52929624 |
| 24 | 11 | 13 | 24.55762068 |
| 25 | 12 | 13 | 63.40922753 |
| 26 | 12 | 16 | 9.977977937 |
| 27 | 12 | 17 | 7.786766182 |
| 28 | 14 | 15 | 41.44628518 |
| 29 | 18 | 19 | 4.964963418 |
| 30 | 19 | 20 | 1.483295923 |
| 31 | 21 | 20 | 1.038667679 |
| 32 | 21 | 22 | 1.039899265 |
| 33 | 22 | 23 | 7.802792852 |
| 34 | 23 | 24 | 5.562666445 |
| 35 | 24 | 25 | 7.504483663 |
| 36 | 24 | 25 | 7.211625764 |
| 37 | 24 | 26 | 16.51189922 |
| 38 | 26 | 27 | 16.92148904 |
| 39 | 27 | 28 | 26.6312403 |
| 40 | 28 | 29 | 31.78793109 |

**TABLE 13.** (Continued.) Transmission Line apparent power:57-bus system.

| | | | |
|---|---|---|---|
| 41 | 7 | 29 | 67.37797222 |
| 42 | 25 | 30 | 9.19061985 |
| 43 | 30 | 31 | 4.98037579 |
| 44 | 31 | 32 | 1.680551292 |
| 45 | 32 | 33 | 4.258851593 |
| 46 | 34 | 32 | 8.014024285 |
| 47 | 34 | 35 | 8.014024287 |
| 48 | 35 | 36 | 14.71042321 |
| 49 | 36 | 37 | 19.17491121 |
| 50 | 37 | 38 | 24.02685148 |
| 51 | 37 | 39 | 4.391465499 |
| 52 | 36 | 40 | 4.9478077 |
| 53 | 22 | 38 | 8.730539415 |
| 54 | 11 | 41 | 10.64039751 |
| 55 | 41 | 42 | 10.39361214 |
| 56 | 41 | 43 | 13.19630125 |
| 57 | 38 | 44 | 15.30274417 |
| 58 | 15 | 45 | 27.77256046 |
| 59 | 14 | 46 | 52.30278549 |
| 60 | 46 | 47 | 51.35826105 |
| 61 | 47 | 48 | 19.64699809 |
| 62 | 48 | 49 | 6.783134971 |
| 63 | 49 | 50 | 8.460242599 |
| 64 | 50 | 51 | 16.95763841 |
| 65 | 10 | 51 | 35.94795015 |
| 66 | 13 | 49 | 47.62053925 |
| 67 | 29 | 52 | 18.00521162 |
| 68 | 52 | 53 | 12.43156727 |
| 69 | 53 | 54 | 8.992942564 |
| 70 | 54 | 55 | 13.73053989 |
| 71 | 11 | 43 | 15.49958321 |
| 72 | 44 | 45 | 27.73201239 |
| 73 | 40 | 56 | 4.933592651 |
| 74 | 56 | 41 | 6.671829826 |
| 75 | 56 | 42 | 3.008889965 |
| 76 | 39 | 57 | 4.382736333 |
| 77 | 57 | 56 | 3.781536498 |
| 78 | 38 | 49 | 11.85791416 |
| 79 | 38 | 48 | 26.20104069 |
| 80 | 9 | 55 | 21.57017417 |

**TABLE 14.** Transmission Line apparent power:118-bus system.

| Transmission Line Number | From bus | To bus | Apparent Power |
|---|---|---|---|
| 1 | 1 | 2 | 16.19516513 |
| 2 | 1 | 3 | 30.9526128 |
| 3 | 4 | 5 | 99.71527581 |
| 4 | 3 | 5 | 58.73353321 |
| 5 | 5 | 6 | 79.64963738 |
| 6 | 6 | 7 | 29.70911681 |
| 7 | 8 | 9 | 407.5454515 |
| 8 | 8 | 5 | 323.9646851 |
| 9 | 9 | 10 | 405.5035341 |
| 10 | 4 | 11 | 56.95215386 |
| 11 | 5 | 11 | 69.09270228 |
| 12 | 11 | 12 | 38.76901495 |
| 13 | 2 | 12 | 32.8936251 |
| 14 | 3 | 12 | 14.82682976 |
| 15 | 7 | 12 | 11.62982977 |
| 16 | 11 | 13 | 33.85633403 |
| 17 | 12 | 14 | 15.54407039 |
| 18 | 13 | 15 | 4.294273769 |
| 19 | 14 | 15 | 8.968240002 |
| 20 | 12 | 16 | 9.943628483 |
| 21 | 15 | 17 | 87.22825731 |
| 22 | 16 | 17 | 17.59960224 |
| 23 | 17 | 18 | 65.6883144 |
| 24 | 18 | 19 | 23.21768165 |
| 25 | 19 | 20 | 4.860452415 |
| 26 | 15 | 19 | 19.1683577 |
| 27 | 20 | 21 | 19.86884336 |
| 28 | 21 | 22 | 34.05890119 |
| 29 | 22 | 23 | 45.29636129 |
| 30 | 23 | 24 | 25.16990732 |
| 31 | 23 | 25 | 160.5869773 |
| 32 | 26 | 25 | 91.56689601 |
| 33 | 25 | 27 | 130.5033238 |
| 34 | 27 | 28 | 31.16349022 |
| 35 | 28 | 29 | 15.25529098 |
| 36 | 30 | 17 | 219.5263666 |
| 37 | 8 | 30 | 96.72403964 |
| 38 | 26 | 30 | 192.7490226 |
| 39 | 17 | 31 | 24.23857992 |
| 40 | 29 | 31 | 12.9805369 |
| 41 | 23 | 32 | 79.89905652 |

**TABLE 14.** *(Continued.)* Transmission Line apparent power:118-bus system.

| | | | |
|---|---|---|---|
| 42 | 31 | 32 | 28.36791103 |
| 43 | 27 | 32 | 14.17317015 |
| 44 | 15 | 33 | 8.286524196 |
| 45 | 19 | 34 | 10.99537127 |
| 46 | 35 | 36 | 7.0228185 |
| 47 | 35 | 37 | 32.18743513 |
| 48 | 33 | 37 | 19.09545575 |
| 49 | 34 | 36 | 23.51082283 |
| 50 | 34 | 37 | 98.69644236 |
| 51 | 38 | 37 | 219.5282678 |
| 52 | 37 | 39 | 31.87189678 |
| 53 | 37 | 40 | 21.17277954 |
| 54 | 30 | 38 | 78.18586291 |
| 55 | 39 | 40 | 3.292341796 |
| 56 | 40 | 41 | 18.29234579 |
| 57 | 40 | 42 | 11.61224054 |
| 58 | 41 | 42 | 20.68399591 |
| 59 | 43 | 44 | 9.497327173 |
| 60 | 34 | 43 | 9.838973342 |
| 61 | 44 | 45 | 25.38097392 |
| 62 | 45 | 46 | 32.20846224 |
| 63 | 46 | 47 | 26.77766433 |
| 64 | 46 | 48 | 15.65541504 |
| 65 | 47 | 49 | 19.38179739 |
| 66 | 42 | 49 | 40.3626348 |
| 67 | 42 | 49 | 40.3626348 |
| 68 | 45 | 49 | 47.71072872 |
| 69 | 48 | 49 | 35.04195061 |
| 70 | 49 | 50 | 49.74450281 |
| 71 | 49 | 51 | 63.22495858 |
| 72 | 51 | 52 | 27.44528481 |
| 73 | 52 | 53 | 10.36197008 |
| 74 | 53 | 54 | 15.45672977 |
| 75 | 49 | 54 | 35.34191782 |
| 76 | 49 | 54 | 34.5760721 |
| 77 | 54 | 55 | 4.838700613 |
| 78 | 54 | 56 | 10.02162102 |
| 79 | 55 | 56 | 12.72330148 |
| 80 | 56 | 57 | 20.75981396 |
| 81 | 50 | 57 | 32.02095049 |
| 82 | 56 | 58 | 6.11921398 |
| 83 | 51 | 58 | 15.3456945 |

**TABLE 14.** *(Continued.)* Transmission Line apparent power:118-bus system.

| | | | |
|---|---|---|---|
| 84 | 54 | 59 | 22.46482219 |
| 85 | 56 | 59 | 19.98181451 |
| 86 | 56 | 59 | 20.81642898 |
| 87 | 55 | 59 | 24.64075774 |
| 88 | 59 | 60 | 35.90069486 |
| 89 | 59 | 61 | 44.27649726 |
| 90 | 60 | 61 | 106.3963528 |
| 91 | 60 | 62 | 10.89257588 |
| 92 | 61 | 62 | 29.66461859 |
| 93 | 63 | 59 | 145.5973309 |
| 94 | 63 | 64 | 145.5973309 |
| 95 | 64 | 61 | 32.35796689 |
| 96 | 38 | 65 | 143.1893783 |
| 97 | 64 | 65 | 171.0836627 |
| 98 | 49 | 66 | 107.7154963 |
| 99 | 49 | 66 | 107.7154963 |
| 100 | 62 | 66 | 39.96683491 |
| 101 | 62 | 67 | 27.34230267 |
| 102 | 65 | 66 | 72.72651769 |
| 103 | 66 | 67 | 55.35263873 |
| 104 | 65 | 68 | 84.223847 |
| 105 | 47 | 69 | 44.90126243 |
| 106 | 49 | 69 | 35.81942779 |
| 107 | 68 | 69 | 154.5347783 |
| 108 | 69 | 70 | 96.91060198 |
| 109 | 24 | 70 | 6.862003298 |
| 110 | 70 | 71 | 15.06433404 |
| 111 | 24 | 72 | 9.98176792 |
| 112 | 71 | 72 | 6.455944587 |
| 113 | 71 | 73 | 12.26236949 |
| 114 | 70 | 74 | 21.37283895 |
| 115 | 70 | 75 | 12.31804669 |
| 116 | 69 | 75 | 102.6648758 |
| 117 | 74 | 75 | 39.67034609 |
| 118 | 76 | 77 | 54.11258118 |
| 119 | 69 | 77 | 73.77393977 |
| 120 | 75 | 77 | 27.20252526 |
| 121 | 77 | 78 | 49.86221263 |
| 122 | 78 | 79 | 29.05365312 |
| 123 | 77 | 80 | 98.17912994 |
| 124 | 77 | 80 | 46.19152188 |
| 125 | 79 | 80 | 69.07846856 |

**TABLE 14.** *(Continued.)* Transmission Line apparent power:118-bus system.

| | | | |
|---|---|---|---|
| 126 | 68 | 81 | 73.82285985 |
| 127 | 81 | 80 | 73.82285985 |
| 128 | 77 | 82 | 25.07300464 |
| 129 | 82 | 83 | 25.90721486 |
| 130 | 83 | 84 | 17.9936233 |
| 131 | 83 | 85 | 27.9360333 |
| 132 | 84 | 85 | 25.50348036 |
| 133 | 85 | 86 | 19.05640115 |
| 134 | 86 | 87 | 15.58164616 |
| 135 | 85 | 88 | 36.74445663 |
| 136 | 85 | 89 | 57.51638769 |
| 137 | 88 | 89 | 85.89202821 |
| 138 | 89 | 90 | 55.06868803 |
| 139 | 89 | 90 | 104.6037201 |
| 140 | 90 | 91 | 12.02313656 |
| 141 | 89 | 92 | 146.953018 |
| 142 | 89 | 92 | 46.51037632 |
| 143 | 91 | 92 | 18.12280678 |
| 144 | 92 | 93 | 37.466052 |
| 145 | 92 | 94 | 33.10581586 |
| 146 | 93 | 94 | 27.93946937 |
| 147 | 94 | 95 | 37.6627461 |
| 148 | 80 | 96 | 34.44477696 |
| 149 | 82 | 96 | 16.14900588 |
| 150 | 94 | 96 | 16.74222185 |
| 151 | 80 | 97 | 42.04694302 |
| 152 | 80 | 98 | 30.55792801 |
| 153 | 80 | 99 | 23.26507845 |
| 154 | 92 | 100 | 19.18570511 |
| 155 | 94 | 100 | 47.16937746 |
| 156 | 95 | 96 | 21.1318425 |
| 157 | 96 | 97 | 25.84866162 |
| 158 | 98 | 100 | 9.020038799 |
| 159 | 99 | 100 | 23.13008622 |
| 160 | 100 | 101 | 20.7888911 |
| 161 | 92 | 102 | 27.18203091 |
| 162 | 101 | 102 | 22.87368762 |
| 163 | 100 | 103 | 73.24426545 |
| 164 | 100 | 104 | 40.3791519 |
| 165 | 103 | 104 | 31.24425523 |
| 166 | 103 | 105 | 35.7526262 |
| 167 | 100 | 106 | 43.00467444 |

**TABLE 14.** *(Continued.)* Transmission Line apparent power:118-bus system.

| 168 | 104 | 105 | 26.60872171 |
|-----|-----|-----|-------------|
| 169 | 105 | 106 | 11.7954862 |
| 170 | 105 | 107 | 13.07257313 |
| 171 | 105 | 108 | 7.755638906 |
| 172 | 106 | 107 | 9.822268319 |
| 173 | 108 | 109 | 5.841663009 |
| 174 | 103 | 110 | 32.7538144 |
| 175 | 109 | 110 | 7.871511259 |
| 176 | 110 | 111 | 35.1106505 |
| 177 | 110 | 112 | 31.77330784 |
| 178 | 17 | 113 | 9.817448254 |
| 179 | 32 | 113 | 16.16327704 |
| 180 | 32 | 114 | 9.267364369 |
| 181 | 27 | 115 | 22.29989701 |
| 182 | 114 | 115 | 0.89797348 |
| 183 | 68 | 116 | 196.4423459 |
| 184 | 12 | 117 | 21.54065923 |
| 185 | 75 | 118 | 44.80351045 |
| 186 | 76 | 118 | 11.72591879 |

**TABLE 15.** Generator capacity limits of 30-bus system.

| Gen. No. | Gen. at bus | $P_{max}$ (MW) |
|----------|-------------|----------------|
| 1 | 1 | 400 |
| 2 | 2 | 80 |
| 3 | 5 | 50 |
| 4 | 8 | 35 |
| 5 | 11 | 30 |
| 6 | 13 | 40 |

**TABLE 16.** Generator capacity limits of 57-bus system.

| Gen. No. | Gen. at bus | $P_{max}$ (MW) |
|----------|-------------|----------------|
| 1 | 1 | 576 |
| 2 | 2 | 100 |
| 3 | 3 | 140 |
| 4 | 6 | 100 |
| 5 | 8 | 550 |
| 6 | 9 | 100 |
| 7 | 12 | 410 |

**TABLE 17.** Generator capacity limits of 118-bus system.

| Gen. No. | Gen. at bus | $P_{max}$ (MW) |
|----------|-------------|----------------|
| 1 | 1 | 100 |
| 2 | 4 | 100 |
| 3 | 6 | 100 |
| 4 | 8 | 100 |
| 5 | 10 | 550 |
| 6 | 12 | 185 |
| 7 | 15 | 100 |
| 8 | 18 | 100 |
| 9 | 19 | 100 |
| 10 | 24 | 100 |
| 11 | 25 | 320 |
| 12 | 26 | 414 |
| 13 | 27 | 100 |
| 14 | 31 | 107 |
| 15 | 32 | 100 |
| 16 | 34 | 100 |
| 17 | 36 | 100 |
| 18 | 40 | 100 |
| 19 | 42 | 100 |
| 20 | 46 | 119 |
| 21 | 49 | 304 |
| 22 | 54 | 148 |
| 23 | 55 | 100 |
| 24 | 56 | 100 |
| 25 | 59 | 255 |
| 26 | 61 | 260 |
| 27 | 62 | 100 |
| 28 | 65 | 491 |
| 29 | 66 | 492 |
| 30 | 69 | 805 |
| 31 | 70 | 100 |
| 32 | 72 | 100 |
| 33 | 73 | 100 |
| 34 | 74 | 100 |
| 35 | 76 | 100 |
| 36 | 77 | 100 |
| 37 | 80 | 577 |
| 38 | 85 | 100 |
| 39 | 87 | 104 |
| 40 | 89 | 707 |
| 41 | 90 | 100 |

**TABLE 17.** (Continued.) Generator capacity limits of 118-bus system.

| 42 | 91 | 100 |
|----|-----|-----|
| 43 | 92 | 100 |
| 44 | 99 | 100 |
| 45 | 100 | 352 |
| 46 | 103 | 140 |
| 47 | 104 | 100 |
| 48 | 105 | 100 |
| 49 | 107 | 100 |
| 50 | 110 | 100 |
| 51 | 111 | 136 |
| 52 | 112 | 100 |
| 53 | 113 | 100 |
| 54 | 116 | 100 |

of parking lot-based charging infrastructures to facilitate the efficient integration of plug-in electric vehicles is presented.

## V. CONCLUSION

This article has proposed an application of the newly developed HOA in solving one of the most vital problems in the field of electric power systems, the OPF problem. The simulation is performed on the standard test systems, the IEEE 30-bus, 57-bus, and 118-bus systems. In the second part of the research, The SFO and HHO algorithms are employed to select optimal buses for inserting PV panel and wind farm into the systems under study. As a final stage, the proposed HOA is used to solve the OPF problem considering different scenarios of renewable power sources integration with the power systems and varying load conditions in the three systems. The simulation results have confirmed the validity, and robustness of the newly developed HOA method compared with the results obtained by GA. The HOA method has extensively shown a higher speed and smoother convergence of the fitness function besides its simplicity in computations and implementation. The application of the HOA has resulted in a 4% reduction in fuel cost for the base case OPF. Meanwhile, in the different scenarios, the HOA has demonstrated a percentage reduction in the daily costs by (0.7-9%) compared with that achieved by the GA results. So, it is recommended to consider using the HOA method in further applications in the field of power system simulations such as smart grids in the future works.

## REFERENCES

[1] Q. Hou, E. Du, N. Zhang, and C. Kang, "Impact of high renewable penetration on the power system operation mode: A data-driven approach," *IEEE Trans. Power Syst.*, vol. 35, no. 1, pp. 731–741, Jan. 2020, doi: 10.1109/TPWRS.2019.2929276.

[2] A. A. Nazari, R. Keypour, M. H. Beiranvand, and N. Amjady, "A decoupled extended power flow analysis based on Newton-Raphson method for islanded microgrids," *Int. J. Electr. Power Energy Syst.*, vol. 117, May 2020, Art. no. 105705, doi: 10.1016/j.ijepes.2019.105705.

[3] W. Lu, M. Liu, S. Lin, and L. Li, "Fully decentralized optimal power flow of multi-area interconnected power systems based on distributed interior point method," *IEEE Trans. Power Syst.*, vol. 33, no. 1, pp. 901–910, Jan. 2018, doi: 10.1109/TPWRS.2017.2694860.

[4] F. E. Fernandes Junior and G. G. Yen, "Particle swarm optimization of deep neural networks architectures for image classification," *Swarm Evol. Comput.*, vol. 49, pp. 62–74, Sep. 2019, doi: 10.1016/j.swevo.2019.05.010.

[5] M. H. Nadimi-Shahraki, S. Taghian, and S. Mirjalili, "An improved grey wolf optimizer for solving engineering problems," *Expert Syst. Appl.*, vol. 166, Mar. 2021, Art. no. 113917, doi: 10.1016/j.eswa.2020.113917.

[6] M. A. M. Shaheen, H. M. Hasanien, and A. Alkuhayli, "A novel hybrid GWO-PSO optimization technique for optimal reactive power dispatch problem solution," *Ain Shams Eng. J.*, Aug. 2020, doi: 10.1016/j.asej.2020.07.011.

[7] I. Gungor, B. G. Emiroglu, A. C. Cinar, and M. S. Kiran, "Integration search strategies in tree seed algorithm for high dimensional function optimization," *Int. J. Mach. Learn. Cybern.*, vol. 11, no. 2, pp. 249–267, Feb. 2020, doi: 10.1007/s13042-019-00970-1.

[8] S. Gupta and K. Deep, "Improved sine cosine algorithm with crossover scheme for global optimization," *Knowl.-Based Syst.*, vol. 165, pp. 374–406, Feb. 2019, doi: 10.1016/j.knosys.2018.12.008.

[9] M. A. M. Shaheen, H. M. Hasanien, S. F. Mekhamer, and H. E. A. Talaat, "Optimal power flow of power systems including distributed generation units using sunflower optimization algorithm," *IEEE Access*, vol. 7, pp. 109289–109300, 2019, doi: 10.1109/ACCESS.2019.2933489.

[10] G. F. Gomes and F. A. de Almeida, "Tuning Metaheuristic algorithms using mixture design: Application of sunflower optimization for structural damage identification," *Adv. Eng. Softw.*, vol. 149, Nov. 2020, Art. no. 102877, doi: 10.1016/j.advengsoft.2020.102877.

[11] A. A. Z. Diab, H. M. Sultan, T. D. Do, O. M. Kamel, and M. A. Mossa, "Coyote optimization algorithm for parameters estimation of various models of solar cells and PV modules," *IEEE Access*, vol. 8, pp. 111102–111140, 2020, doi: 10.1109/ACCESS.2020.3000770.

[12] H. Chen, S. Jiao, M. Wang, A. A. Heidari, and X. Zhao, "Parameters identification of photovoltaic cells and modules using diversification-enriched harris hawks optimization with chaotic drifts," *J. Cleaner Prod.*, vol. 244, Jan. 2020, Art. no. 118778, doi: 10.1016/j.jclepro.2019.118778.

[13] M. A. M. Shaheen, H. M. Hasanien, S. F. Mekhamer, and H. E. A. Talaat, "Optimal power flow of power networks with penetration of renewable energy sources by harris hawks optimization method," in *Proc. 2nd Int. Conf. Smart Power Internet Energy Syst. (SPIES)*, Sep. 2020, pp. 537–542, doi: 10.1109/SPIES48661.2020.9242932.

[14] A. M. Hussien, S. F. Mekhamer, and H. M. Hasanien, "Cuttlefish optimization algorithm based optimal PI controller for performance enhancement of an autonomous operation of a DG system," in *Proc. 2nd Int. Conf. Smart Power Internet Energy Syst. (SPIES)*, Sep. 2020, pp. 293–298, doi: 10.1109/SPIES48661.2020.9243093.

[15] R. N. Kalaam, S. M. Muyeen, A. Al-Durra, H. M. Hasanien, and K. Al-Wahedi, "Optimisation of controller parameters for grid-tied photovoltaic system at faulty network using artificial neural network-based cuckoo search algorithm," *IET Renew. Power Gener.*, vol. 11, no. 12, pp. 1517–1526, Oct. 2017, doi: 10.1049/iet-rpg.2017.0040.

[16] O. S. Elazab, H. M. Hasanien, M. A. Elgendy, and A. M. Abdeen, "Parameters estimation of single-and multiple-diode photovoltaic model using whale optimisation algorithm," *IET Renew. Power Gener.*, vol. 12, no. 15, pp. 1755–1761, Nov. 2018, doi: 10.1049/iet-rpg.2018.5317.

[17] H. M. Hasanien, "Gravitational search algorithm-based optimal control of archimedes wave swing-based wave energy conversion system supplying a DC microgrid under uncertain dynamics," *IET Renew. Power Gener.*, vol. 11, no. 6, pp. 763–770, May 2017, doi: 10.1049/iet-rpg.2016.0677.

[18] M. A. M. Shaheen, D. Yousri, A. Fathy, H. M. Hasanien, A. Alkuhayli, and S. M. Muyeen, "A novel application of improved marine predators algorithm and particle swarm optimization for solving the ORPD problem," *Energies*, vol. 13, no. 21, p. 5679, Oct. 2020, doi: 10.3390/en13215679.

[19] H. M. Hasanien and A. A. El-Fergany, "Salp swarm algorithm-based optimal load frequency control of hybrid renewable power systems with communication delay and excitation cross-coupling effect," *Electr. Power Syst. Res.*, vol. 176, Nov. 2019, Art. no. 105938, doi: 10.1016/j.epsr.2019.105938.

[20] L. Abualigah, M. Shehab, M. Alshinwan, and H. Alabool, "Salp swarm algorithm: A comprehensive survey," *Neural Comput. Appl.*, vol. 15, pp. 1–21, Nov. 2019, doi: 10.1007/s00521-019-04629-4.

[21] A. A. El-Fergany and H. M. Hasanien, "Salp swarm optimizer to solve optimal power flow comprising voltage stability analysis," *Neural Comput. Appl.*, vol. 32, no. 9, pp. 5267–5283, May 2020, doi: 10.1007/s00521-019-04029-8.

[22] O. S. Elazab, M. Debouza, H. M. Hasanien, S. M. Muyeen, and A. Al-Durra, "Salp swarm algorithm-based optimal control scheme for LVRT capability improvement of grid-connected photovoltaic power plants: Design and experimental validation," *IET Renew. Power Gener.*, vol. 14, no. 4, pp. 591–599, Mar. 2020, doi: 10.1049/iet-rpg.2019.0726.

[23] A. H. Halim, I. Ismail, and S. Das, "Performance assessment of the metaheuristic optimization algorithms: An exhaustive review," *Artif. Intell. Rev.*, vol. 7, pp. 1–87, Oct. 2020, doi: 10.1007/s10462-020-09906-6.

[24] Q. Askari, M. Saeed, and I. Younas, "Heap-based optimizer inspired by corporate rank hierarchy for global optimization," *Expert Syst. Appl.*, vol. 161, Dec. 2020, Art. no. 113702, doi: 10.1016/j.eswa.2020.113702.

[25] M. Mousa, M. M. Salah, F. Z. Amer, A. Saeed, and R. I. Mubarak, "High efficiency tandem Perovskite/CIGS solar cell," in *Proc. 2nd Int. Conf. Smart Power Internet Energy Syst. (SPIES)*, Sep. 2020, pp. 224–227, doi: 10.1109/SPIES48661.2020.9242927.

[26] M. A. Soliman, H. M. Hasanien, H. Z. Azazi, E. E. El-kholy, and S. A. Mahmoud, "Hybrid ANFIS-GA-based control scheme for performance enhancement of a grid-connected wind generator," *IET Renew. Power Gener.*, vol. 12, no. 7, pp. 832–843, May 2018, doi: 10.1049/iet-rpg.2017.0576.

[27] M. A. Soliman, H. M. Hasanien, S. Alghuwainem, and A. Al-Durra, "Symbiotic organisms search algorithm-based optimal control strategy for efficient operation of variable-speed wind generators," *IET Renew. Power Gener.*, vol. 13, no. 14, pp. 2684–2692, Oct. 2019, doi: 10.1049/iet-rpg.2019.0834.

[28] H. Li, X. Xie, A. McDonald, Z. Chai, T. Yang, Y. Wu, and W. Yang, "Cost and reliability optimization of modular multilevel converter with hybrid submodule for offshore DC wind turbine," *Int. J. Electr. Power Energy Syst.*, vol. 120, Sep. 2020, Art. no. 105994, doi: 10.1016/j.ijepes.2020.105994.

[29] F. Islam, H. Hasanien, A. Al-Durra, and S. M. Muyeen, "A new control strategy for smoothing of wind farm output using short-term ahead wind speed prediction and flywheel energy storage system," in *Proc. Amer. Control Conf. (ACC)*, Jun. 2012, pp. 3026–3031, doi: 10.1109/ACC.2012.6315503.

[30] A. Parida and B. Subudhi, "Modified leaky LMS-based control strategy for reliable operation of single-stage three-phase grid-tied PV system," *IET Renew. Power Gener.*, vol. 14, no. 9, pp. 1453–1462, Jul. 2020, doi: 10.1049/iet-rpg.2019.0776.

[31] G. Wu, C. Zhang, C. Cai, K. Yang, and K. Shi, "Uncertainty prediction on the angle of attack of wind turbine blades based on the field measurements," *Energy*, vol. 200, Jun. 2020, Art. no. 117515, doi: 10.1016/j.energy.2020.117515.

[32] MATPOWER. *The Newton-Raphson Method*. Accessed: Jan. 2020. [Online]. Available: http://www.pserc.cornell.edu/matpower

[33] S. S. Reddy, "Optimal scheduling of thermal-wind-solar power system with storage," *Renew. Energy*, vol. 101, pp. 1357–1368, Feb. 2017.

[34] S. Surender Reddy, P. R. Bijwe, and A. R. Abhyankar, "Optimal posturing in day-ahead market clearing for uncertainties considering anticipated real-time adjustment costs," *IEEE Syst. J.*, vol. 9, no. 1, pp. 177–190, Mar. 2015, doi: 10.1109/JSYST.2013.2265664.

[35] S. S. Reddy, V. Sandeep, and C. M. Jung, "Review of stochastic optimization methods for smart grid," *Frontiers Energy*, vol. 11, no. 2, pp. 197–209, 2017.

[36] S. S. Reddy, D. of Railroad, and R. o. K. Electrical EngineeringWoosong UniversityDaejeon-300718, "Optimization of renewable energy resources in hybrid energy systems," *J. Green Eng.*, vol. 7, no. 1, pp. 43–60, 2017, doi: 10.13052/jge1904-4720.7123.

[37] S. Gill, I. Kockar, and G. W. Ault, "Dynamic optimal power flow for active distribution networks," *IEEE Trans. Power Syst.*, vol. 29, no. 1, pp. 121–131, Jan. 2014, doi: 10.1109/TPWRS.2013.2279263.

[38] J. Medina, N. Muller, and I. Roytelman, "Demand response and distribution grid operations: Opportunities and challenges," *IEEE Trans. Smart Grid*, vol. 1, no. 2, pp. 193–198, Sep. 2010, doi: 10.1109/TSG.2010.2050156.

[39] B. Zeng, J. Feng, N. Liu, and Y. Liu, "Co-optimized parking lot placement and incentive design for promoting PEV integration considering decision-dependent uncertainties," *IEEE Trans. Ind. Informat.*, vol. 17, no. 3, pp. 1863–1872, Mar. 2021, doi: 10.1109/TII.2020.2993815.

[40] B. Zeng, Y. Liu, F. Xu, Y. Liu, X. Sun, and X. Ye, "Optimal demand response resource exploitation for efficient accommodation of renewable energy sources in multi-energy systems considering correlated uncertainties," *J. Cleaner Prod.*, vol. 288, Mar. 2021, Art. no. 125666, doi: 10.1016/j.jclepro.2020.125666.

**MOHAMED A. M. SHAHEEN** received the B.Sc. and M.Sc. degrees in electrical engineering from Ain Shams University, Faculty of Engineering, Cairo, Egypt, in 2016 and 2020, respectively, where he is currently pursuing the Ph.D. degree. He is currently an Assistant Lecturer with the Future University in Egypt, Faculty of Engineering. His research interests include power systems operation, energy storage systems, and renewable energy systems.

**HANY M. HASANIEN** (Senior Member, IEEE) received the B.Sc., M.Sc., and Ph.D. degrees in electrical engineering from Ain Shams University, Faculty of Engineering, Cairo, Egypt, in 1999, 2004, and 2007, respectively. From 2008 to 2011, he was a Joint Researcher with the Kitami Institute of Technology, Kitami, Japan. From 2012 to 2015, he was an Associate Professor with the College of Engineering, King Saud University, Riyadh, Saudi Arabia. He is currently a Professor with the Electrical Power and Machines Department, Faculty of Engineering, Ain Shams University. He has authored, coauthored, and edited three books in the field of electric machines and renewable energy. He has published more than 150 papers in international journals and conferences. His biography has been included in *Marquis Who's Who in the world* for its 28 edition, 2011. His research interests include modern control techniques, power systems dynamics and control, energy storage systems, renewable energy systems, and smart grid. He is an Editorial Board Member of *Electric Power Components and Systems Journal*. He is the Subject Editor of the *IET Renewable Power Generation*, *Ain Shams Engineering Journal*, and *Electronics MDPI*. He was awarded the Encouraging Egypt Award for Engineering Sciences in 2012. He was awarded the Institutions Egypt Award for Invention and Innovation of Renewable Energy Systems Development in 2014. He was awarded the Superiority Egypt Award for Engineering Sciences in 2019. He is currently the IEEE PES Egypt Chapter Chair.

**AHMED AL-DURRA** (Senior Member, IEEE) received the Ph.D. degree in ECE from Ohio State University in 2010. He is currently a Professor with the EECS Department, Khalifa University, UAE. His research interests are applications of control and estimation theory on power systems stability, micro and smart grids, renewable energy systems and integration, and process control. He has one US patent, one edited book, 12 book chapters, and over 210 scientific articles in top-tier journals and refereed international conference proceedings. He has supervised/co-supervised over 25 Ph.D./master's students. He is leading the Energy Systems Control & Optimization Lab under the Advanced Power & Energy Center, an Editor for the IEEE TRANSACTIONS ON SUSTAINABLE ENERGY and IEEE POWER ENGINEERING LETTERS, and an Associate Editor for the IEEE TRANSACTIONS ON INDUSTRY APPLICATIONS, *IET Renewable Power Generation*, and *Frontiers in Energy Research*.

● ● ●